Characterization of PBL height and structure by Raman lidar: Selected case studies from the convective and orographically-induced precipitation study

Donato Summa, Paolo Di Girolamo, and Dario Stelitano

Citation: AIP Conference Proceedings **1531**, 208 (2013); doi: 10.1063/1.4804743
View online: http://dx.doi.org/10.1063/1.4804743
View Table of Contents: http://scitation.aip.org/content/aip/proceeding/aipcp/1531?ver=pdfcov
Published by the AIP Publishing

Characterization of PBL Height and Structure by Raman Lidar: Selected Case Studies from the Convective and Orographically-induced Precipitation Study

Donato Summa, Paolo Di Girolamo and Dario Stelitano

DIFA, Univ. della Basilicata, Viale dell'Ateneo Lucano n. 10, 85100 Potenza, Italy, phone: +39-0971-205134, fax: +39-0971-205160, e-mail: digirolamo@unibas.it, summa@unibas.it, dario.steliatno@unbas.it

Abstract. The planetary boundary layer includes the portion of the atmosphere which is directly influenced by the presence of the Earth's surface. Aerosol particles trapped within the PBL can be used as tracers to study boundary-layer vertical structure and time variability. The PBL height and structure can be estimated based on the use of Raman lidar data. A first method is based on the first order derivative of the range-corrected elastic signal (RCS). Estimates of the PBL height and structure obtained from the above mentioned approach are compared with simultaneous estimates obtained from potential temperature profiles determined from the radiosondes launched simultaneously to lidar operation. Additional estimates of the boundary layer height are obtained from rotational Raman lidar signals used for temperature measurements signals, this latter approach being preferable in the decaying phase of the boundary layer, when effectiveness of the approach based on the elastic lidar signals may be altered by the presence of the residual layer. Preliminary results and correlation are illustrated and discussed.

Keywords: Boundary Layer, Raman Lidar, Aerosol, Particle backscatter.
PACS: 92.60.e, 92.60.H, 42.68.Wt

INTRODUCTION

The planetary boundary layer (PBL), the lower region of the atmosphere in direct contact with the Earth's surface and is directly influenced by this surface. In this layer physical quantities such as flow velocity, temperature, moisture etc., display rapid fluctuations (turbulence) and vertical mixing is strong.

The characterization of planetary boundary layer is of primary importance in a variety of fields as weather forecasting, climate change modelling and air quality prediction [1, 2]. Aerosol particles are trapped within the PBL and can be used as tracers to study boundary-layer vertical structure and time variability. Aerosols can also be dispersed out of the PBL during strong convection or temporary breaks of the capping temperature inversion. Therefore aerosol backscattered signals collected by lidar systems can be used to determine the height and the internal structure of the PBL [3, 4]. Several methods have been applied to estimate PBL height from lidar signals in the presence of mixed, stable and residual boundary [4–8]. However, the complexity of the phenomena occurring within the PBL and the influence of advection and local accumulation processes in many cases prevent unambiguous determination of PBL height from lidar signals, especially when aerosol stratifications are present within the PBL. The present works aims to compare different approaches to characterize the PBL height and structure based on the data provided by a Raman lidar system with aerosol, water vapor and temperature measurement capability. A method based on the first order derivative of the range-corrected elastic signal, which is a modified version of the method defined by Seibert and Sicard is considered and compared with simultaneous estimates obtained from potential temperature profiles determined from radiosonde data and with estimates obtained from rotational Raman lidar e signals.

BASIL

The University of BASILicata Raman Lidar system (BASIL) was deployed in Achern (Black Forest, Germany, Lat: 48.64 °N, Long: 8.06 °E, Elev.: 140 m) in the frame of the Convective and Orographically-induced Precipitation Study [9, 10]. The COPS experiment was held in Southern Germany and Eastern France in the period 01 June - 31 August 2007, as part of the German Research Foundation (DFG) Priority Program 1167 “Quantitative Precipitation Forecast, with the overarching goal of advancing the quality of forecasts of orographically induced convective precipitation by four-dimensional observations and modelling of its life cycle [11–13]. During COPS,

Radiation Processes in the Atmosphere and Ocean (IRS2012)
AIP Conf. Proc. 1531, 208-211 (2013); doi: 10.1063/1.4804743

BASIL operated between 25 May and 30 August 2007 and collected more than 500 hours of measurements, distributed over 58 measurement days and 34 intensive observation periods (IOPs). Quick-looks of the data are available on the COPS Website (http://www.cops2007.de/), under Operational Products, while data for the most important IOPs can be downloaded from the World Data Center for Climate (http://cera-www.dkrz.de/WDCC/ui/BrowseExperiments.jsp?proj=COPS). All other data can be requested directly to the authors of this paper. The major feature of BASIL is represented by its capability to perform high-resolution and accurate measurements of atmospheric temperature and water vapor, both in daytime and night-time, based on the application of the rotational and vibrational Raman lidar techniques in the UV [14–17]. Besides temperature and water vapor, BASIL provides measurements of the particle backscattering coefficient at 355, 532 and 1064 nm, of the particle extinction coefficient at 355 and 532 nm and of particle depolarization at 355 and 532 nm [18, 19].

RESULTS

The algorithm used in this work consider the quantity:

$$D(z) = \frac{d}{dz}(\ln[P_\lambda(z)z^2]) \qquad (1)$$

where $P_\lambda(z)$ is the elastic lidar signal and the quantity $P_\lambda(z)\,z^2$ represents the range correct signal. The minima of the quantity $D(z)$ identify the transitions between different layers. The first minimum usually identifies the boundary layer height. This approach is named as "approach 1" in what follows. For the purpose of this study, expression (1) was applied to the elastic lidar signals at 1064 nm, because of the larger sensitivity of this wavelength to aerosols and their variability. Potential temperature profiles, $T_{pot}(z)$, obtained from the radiosonde data, can also be used to get additional estimates of the boundary layer height. The approach considers the first maximum of the derivative of $T_{pot}(z)$, which identifies the height of its maximum gradient. In the present paper we are also testing an additional approach for the estimate of the boundary layer height based on the application of expression (1) to the rotational Raman signals used to quantify atmospheric temperature (approach 2). In this regard, we need to recall that temperature measurements are performed by *BASIL* through the application of the rotational Raman lidar technique in the UV, which is based on the detection of pure rotational Raman scattering from oxygen and nitrogen molecules in the proximity of the laser wavelength ($P_{\lambda_{Loj}}(z)$ and $P_{\lambda_{Hij}}(z)$). Atmospheric temperature can be obtained from the power ratio of high-to-low quantum number rotational Raman signals. Both $P_{\lambda_{Loj}}(z)$ and $P_{\lambda_{Hij}}(z)$ are characterized by a strong sensitivity to temperature variations, the variability being anyhow larger for the signal $P_{\lambda_{Loj}}(z)$ than for the signal $P_{\lambda_{Hij}}(z)$. In the approach 2 considered in the present paper expression (1) is applied to the rotational Raman signal $P_{\lambda_{Loj}}(z)$.

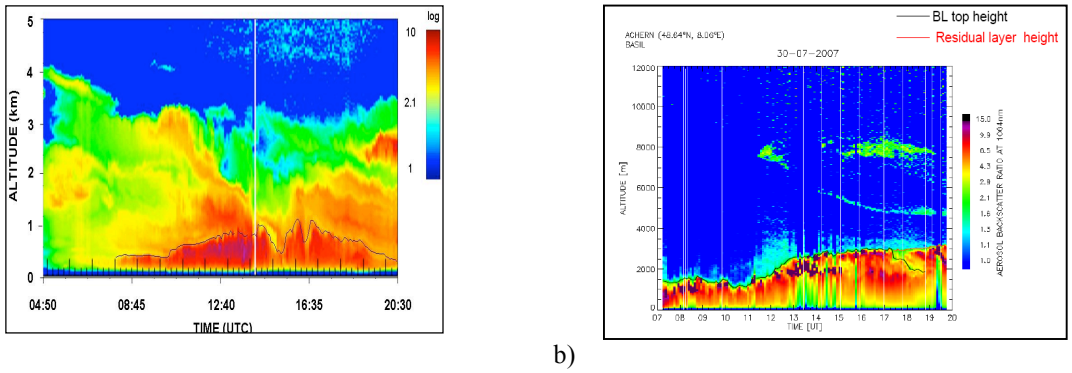

a) b)

FIGURE 1. a) Time evolution of the particle backscattering ratio at 1064 nm as measured by BASIL from 04:50 to 20:00 UT on 15 July 2007. The black line in the figure represents the PBL height as determined through the application of approach 1.b) Time evolution of the particle backscattering ratio at 1064 nm as measured by BASIL from 07:15 to 19:45 UT on 30 July 2007.

Figure 1a-b illustrates the lidar measurements of the particle backscattering ratio at 1064 nm on 15 July 2007 and 30 July, respectively. The black line in this figure represents the PBL height as determined through the application of approach 1, with the red showing also the residual layer obtained from this same algorithm. Figure 2a illustrates the evolution of the boundary layer height as obtained from approach 1 and 2 and the radiosonde data on 15, 25 and 30 July 2007 while in the figure 2b we have compared the outcome of the different algorithm based on the application of a least-square fit analysis. Specifically, the left portion of figure 2b illustrated a liner fit of the PBL estimates from approach 1 versus those obtained from the radiosonde data, while the right portion of the figure illustrated a linear fit of the PBL estimates from approach 2 versus those obtained from the radiosonde data, with the correlation coefficients for the two fits being R=0.97 and R=0.96, respectively.

Figure 2 covers the complete cycle of PBL evolution with both night-time and daytime sectors and the transitions between the two. For all cases the PBL height is found to grow during the day, reaching a maximum value in the early afternoon and then decaying later in the afternoon and evening. In the figure the continuous lines identify the estimates obtained from approach 1, while the yellow stars represent the estimates obtained from the potential temperature profiles of the radiosondes and the blue squares represent the estimates obtained from approach 2.

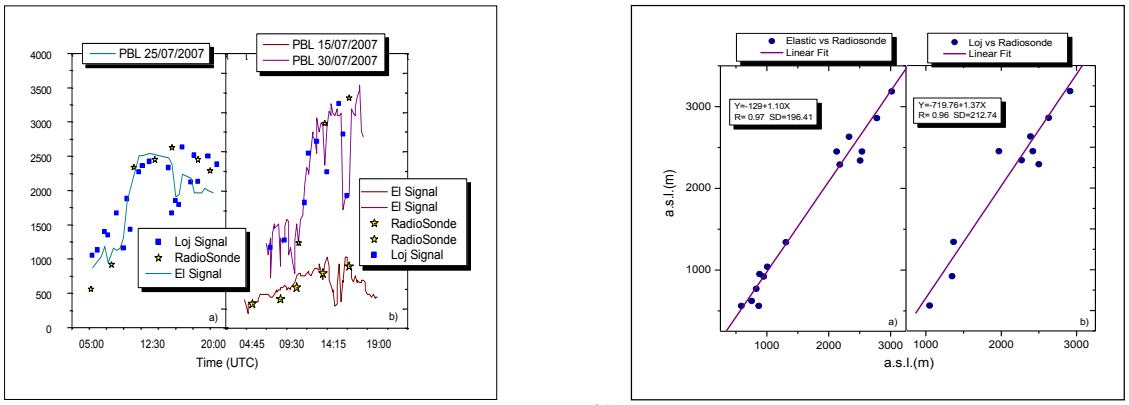

a) b)

FIGURE 2. Panel a: evolution of the PBL height for 15, 25 and 30 July 2007. The continuous lines identify the PBL height estimates obtained from approach 1. Green line is 25 July in the right of panel, brown line is 15 July and pink line is 30 July. The yellow stars represent the estimates obtained from the radiosonde potential temperature profiles. The squares represent the estimates obtained from approach(2). Panel b: on the left, PBL estimates from approach 1 versus those obtained from the radiosonde data, and on the right, PBL estimates from approach 2 versus those obtained from the radiosonde data. The figure also illustrates the best fit lines for these datasets with their errors.

For the purpose of the application of approaches 1 and 2, for the signals $P_{\lambda}(z)$ and $P_{\lambda_{Loj}}(z)$ we used an integration time of 30 min and a vertical resolution is 300 m, which allowed to reduce signal statistical fluctuations which could affect their applicability. It is to be noticed the good agreement between the different approaches, with deviations between the different estimates never exceeding 200 m. These results support us on the applicability of the present techniques and the possibility to apply them to different case study characterized by different meteorological conditions.

CONCLUSION

The present work compares estimates of the PBL height for specific case studies as obtained from three distinct methods. The first approach (approach 1) considers a method based on the first order derivative of the range-corrected elastic signal. Potential temperature profiles, $T_{pot}(z)$, obtained from the radiosondes launched simultaneously to lidar operation are also used to get additional estimates of the boundary layer height. Additional estimates of the boundary layer height and structure are obtained from rotational Raman lidar signals (approach 2). These good agreement between the different approaches support us on the applicability of the present techniques and the possibility to apply them to different case study characterized by different meteorological conditions. In this respect, the dataset collected by BASIL during COPS provides a unique source of information for the study of the boundary layer structure and evolution.

REFERENCES

1. S. H. Melfi, J. D. Spinhirne, S. H. Chou and S. P. Palm, *J. Climate Appl. Meteorol.* **24**: 806-821 (1985).
2. Y. J. Kaufmann, D. Tanre and O. Boucher, *Nature*, **419**: 215–223 (2002).
3. P. Seibert, F. Beyrich, S. E. Gryning, S. Joffre, A. Rasmussen and P. Tercier, *Atmos. Environ*. **34**: 1001-1020 (2000).
4. M. Sicard, C. Pérez, F. Rocadembosch, J. M. Baldasano and D. Garcìa-Vizcaino, *Boundary Layer Meteorology* **119** (1): 135-157 (2006).
5. C. Flamant, J. Pelon, P. H. Flamant and P. Durand, *Boundary-Layer Meteorol*. **83**: 247-284 (1997).
6. R. Boers, J. D. Spinhirne and W. D. Hart, *J. Appl. Meteorol*. **27**: 797-810 (1988).
7. W. P. Hooper and E. W. Eloranta, *J. Climate Appl. Meteorol*. **25**: 990-1001 (1986).
8. K. L. Hayden, K. G. Anlauf, R. M. Hoff, J. W. Strapp, J. W. Bottenheim, H. A. Wiebe, F. A. Froude, J. B. Martin, D. G. Steyn and I. G. McKendry, *J. Atmos. Environ*. **31**: 2089–2105 (1997).
9. E. Richard, C. Flamant, F. Bouttier, J. Van Baelen, C. Champollion, M. Hagen, J. Cuesta, P. Bosser, G. Pigeon, S. Argence, J. Arnault, P. Brousseau, Y. Seity, J.-P. Chaboureau, P. Limnaios, F. Masson, Y. Pointin, P. Di Girolamo and V. Wulfmeyer, *La Météorologie* **64**, 32-42 (2009).
10. V. Wulfmeyer, A. Behrendt, H. S. Bauer, C. Kottmeier, U. Corsmeier, A. Blyth, G. Craig, U. Schumann, M. Hagen, S. Crewell, P. Di Girolamo, C. Flamant, M. Miller, A. Montani, S. Mobbs, E. Richard, M. W. Rotach, M. Arpagaus, H. Russchenberg, P. Schlüssel, M. König, V. Gärtner, R. Steinacker, M. Dorninger, D. D. Turner, T. Weckwerth, A. Hense and C. Simmer, *Bulletin of the American Meteorological Society* **89**, 10, 1477-1486 (2008).
11. C. Kottmeier, N. Kalthoff, C. Barthlott, U. Corsmeier, J. Van Baelen, A. Behrendt, R. Behrendt, A. Blyth, R. Coulter, S. Crewell, P. Di Girolamo, M. Dorninger, C. Flamant, T. Foken, M. Hagen, C. Hauck, H. Höller, H. Konow, M. Kunz, H. Mahlke, S. Mobbs, E. Richard, R. Steinacker, T. Weckwerth, A. Wieser and V. Wulfmeyer, *Meteorologische Zeitschrift* **17**, 6, 931-948 (2008).
12. N. Kalthoff, B. Adler, C. Barthlott, U. Corsmeier, S. Mobbs, S. Crewell, K. Trumner, C. Kottmeier, A. Wieser, V. Smith and P. Di Girolamo, *Atmospheric Research*, Ed. Elsevier, **93**, 680-694 (2009).
13. V. Wulfmeyer, A. Behrendt, C. Kottmeier, U. Corsmeier, C. Barthlott, G. C. Craig, M. Hagen, D. Althausen, F. Aoshima, M. Arpagaus, H. S. Bauer, L. Bennett, A. Blyth, C. Brandau, C. Champollion, S. Crewell, G. Dick, P. Di Girolamo, M. Dorninger, Y. Dufournet, R. Eigenmann, R. Engelmann, C. Flamant, T. Foken, T. Gorgas, M. Grzeschik, J. Handwerker, C. Hauck, H. Höller, W. Junkermann, N. Kalthoff, C. Kiemle, S. Klink, M. König, L. Krauss, C. N. Long, F. Madonna, S. Mobbs, B. Neininger, S. Pal, G. Peters, G. Pigeon, E. Richard, M. W. Rotach, H. Russchenberg, T. Schwitalla, V. Smith, R. Steinacker, J. Trentmann, D. D. Turner, J. van Baelen, S. Vogt, H. Volkert, T. Weckwerth, H. Wernli, A. Wieser and M. Wirth, *Quarterly Journal of the Royal Meteorological Society* **137**: 3–30 (2011).
14. P. Di Girolamo, R. Marchese, D. N. Whiteman and B. B. Demoz, *Geophysical Research Letters* **31**, L01106 (2004).
15. P. Di Girolamo, A. Behrendt and V. Wulfmeyer, *Applied Optics* **45**, 11, 2474-2494 (2006).
16. P. Di Girolamo, D. Summa and R. Ferretti, *Journal of Atmospheric and Oceanic Technology* **26**, 9, 1742–1762 (2009).
17. R. Bhawar, P. Di Girolamo, D. Summa, C. Flamant, D. Althausen, A. Behrendt, C. Kiemle, P. Bosser, M. Cacciani, C. Champollion, T. Di Iorio, R. Engelmann, C. Herold, D. Müller, S. Pal, M. Wirth and V. Wulfmeyer, *Quarterly Journal of the Royal Meteorological Society* **137**: 325–348 (2011).
18. P. Di Girolamo, D. Summa, R. F. Lin, T. Maestri, R. Rizzi and G. Masiello, *Atmospheric Chemistry and Physics* **9**, 8799-8811 (2009).
19. T. Maestri, P. Di Girolamo, D. Summa and R. Rizzi, *Atmos. Res.* **97**, 157–169 (2010).